JOURNAL OF CATALYSIS **141**, 368–379 (1993)

A New Procedure for Particle Size Determination by EXAFS Based on Molecular Dynamics Simulations

BJERNE S. CLAUSEN,* LARS GRÅBÆK,* HENRIK TOPSØE,* LARS B. HANSEN,†
PER STOLTZE,† JENS K. NØRSKOV,† AND OLE H. NIELSEN‡

**Haldor Topsøe Research Laboratories, DK-2800 Lyngby, Denmark; †Physics Department, Technical University of Denmark, DK-2800 Lyngby, Denmark; and Uni-C, ‡Technical University of Denmark, DK-2800 Lyngby, Denmark*

Received July 13, 1992; revised December 15, 1992

We present here a new model that allows a more accurate determination of average coordination numbers and metal particle sizes from an EXAFS experiment. The model is based on a set of molecular dynamics simulations of small Cu particles with the total number of atoms ranging from 256 to 17000 (corresponding to particle diameters from about 1.7 to 7.0 nm). The atomic motion in small particles is very anharmonic even at low temperatures, giving rise to asymmetric pair distribution functions with broad tails. It is shown that the standard EXAFS analysis of such particles will typically underestimate the coordination numbers substantially, and the particle size derived from EXAFS therefore in general will be too small. The size of the errors has been evaluated for some of the most common EXAFS analysis procedures suggested in the literature, and it is shown how the new model can provide more reliable particle sizes. The reliability of the new approach is confirmed by comparing simultaneous *in situ* EXAFS and XRD experiments of reduced Cu/SiO$_2$ catalysts. © 1993 Academic Press, Inc.

1. INTRODUCTION

Measurements of particle sizes and surface areas are central in catalysis research. For example, in order to compare catalytic activities of different catalysts, these are normally expressed as turnover frequencies (i.e., the rate of molecules produced per active site). Such comparisons therefore require reliable methods for determination of the surface area (or number of sites) of the active phase in a catalyst. If the surface area is not directly available, it is often estimated from determinations of the particle sizes. Of direct or indirect methods, one could mention volumetric gas chemisorption, X-ray diffraction (XRD), electron microscopy (EM), and various spectroscopies [see, e.g., Refs. (*1*, *2*)]. For highly dispersed systems, where XRD fails to reveal much information, extended X-ray absorption fine structure (EXAFS) has gained widespread use, not only as a general structural characterization technique, but also more specifically for determination of the particle size.

Particles smaller than about 100 Å (10 nm) have a significant fraction of the atoms located at the surface, and the radial distribution function will show a reduction in the coordination numbers. Various models have been proposed [see, e.g., Ref. (*3*, *4*)] to relate EXAFS coordination numbers to metal particle sizes. In general, such relations will depend on the particle shape, which is often unknown, and the models therefore typically assume simple geometrical particle shapes, like spheres, cubes, or discs.

In the literature there are many examples of studies of highly dispersed and/or disordered systems where the EXAFS results are in apparent disagreement with results obtained by other techniques [see, e.g., Refs. (*5*–*8*)]. It is normally assumed that the EXAFS technique is capable of determining structural parameters, like bond lengths and coordination numbers, quite

0021-9517/93 $5.00

accurately in unknown compounds. It is, however, also recognized that large disorder may introduce significant errors in the determination of these parameters [see, e.g., Refs. (*9–14*)]. For example, in an analysis of EXAFS spectra of supported, 10-Å large Pt particles recorded at various temperatures, Marques *et al.* (*11*) observed an apparent bond contraction with increasing temperature. In accordance with earlier work on other disordered systems, this was attributed to the incomplete theoretical treatment of EXAFS spectra for structures with non-Gaussian pair distribution functions.

The estimate of the particle size by EXAFS relies on an accurate determination of the average coordination numbers for the different neighboring atomic shells, and it should be noted that even relatively small errors in the coordination numbers may result in substantial errors in the estimated particle sizes. For example, if the average first shell coordination number is determined to be 10 for a particle with fcc structure, then 10% errors in the determination would result in particle diameters that could be anywhere from 10 to 50 Å. Thus, there is a great need for improved methods to analyze EXAFS spectra with non-Gaussian pair distribution functions.

In a recent study (*15*), we used molecular dynamics simulations to show that the bond length for Cu particles with a total number of atoms between 100 and 1000 changes only very little with particle size. However, the atomic motion in the small particles was found to be very anharmonic and in Ref. (*15*), it was shown that this anharmonicity may introduce significant errors in the apparent bond distance when determined by use of the standard EXAFS analysis, which assumes that the thermal vibrations are harmonic. In the present study, we estimate how the anharmonicity influences the apparent EXAFS coordination number and the molecular dynamics simulations have for this purpose been extended to Cu particles with up to 17000 atoms. On the basis of the simulations, we have deduced relationships between the apparent EXAFS coordination numbers (determined from various analysis procedures) and the "true" coordination numbers. Since the molecular dynamics simulations also give the equilibrium shape of the small particles, the coordination numbers can be related directly to the particle diameters. We have finally applied the model to a set of measurements on catalysts consisting of small Cu particles supported on a silica. In order to test the reliability of the model for estimating coordination numbers (and particle sizes) from EXAFS, *in situ* XRD measurements have been performed in a newly developed setup that allows combined XRD/EXAFS experiments on the *same* sample.

In the present report, we discuss how the results from various EXAFS analysis procedures can be corrected to yield more reliable coordination numbers (and particle sizes). The more detailed aspects of the influence of the specific analysis procedures, like *k*-weighting of the data and truncation at low *k*-values, are discussed in Ref. (*16*).

2. EXPERIMENTAL

a. Sample Preparation

Silica (Wacker HDK fumed silica, s.a. 180 m^2/g)-supported Cu catalysts with various copper concentrations were prepared via precipitation of copper(II) by a homogeneous increase of the hydroxyl ion concentration by the slow hydrolysis of urea at 353 K according to the procedure of Geus and co-workers (*17*). After repeated washings in water and subsequent drying, the catalysts were loaded in the *in situ* cell described below. The activation of the catalysts was carried out in this cell by flowing an argon gas containing 4% H_2, 0.5% CO, and 4% CO_2 over the catalyst, while increasing the temperature gradually from room temperature to the final reduction temperature of 493 K. A sintered sample was prepared by a reduction, oxidation, and rereduction sequence of the 5% Cu/ SiO_2 catalyst. The oxidation was carried out in air at 500 K for 2 h, whereas the rereduction followed the normal reduction scheme.

b. Combined XRD/EXAFS Measurements

The XRD/EXAFS experiments were performed at HASLAB and DESY (Hamburg, Germany). The data were obtained using the synchrotron radiation from the DORIS III storage ring and the RÖMO II experimental station. Two parallel Si(311) crystals were used to monochromatize the X-ray beam. The content of higher harmonics in the monochromatized beam was removed by slightly detuning the crystals from parallel and the intensity of the incident and transmitted X rays was recorded by use of N_2-filled ionization chambers. The *in situ* cell (*18*) was a quartz tube with an outer diameter of 0.5 mm and a wall thickness of 0.01 mm. By use of narrow slits, these tubes can be used equally well as sample holders for XRD and for EXAFS in the transmission mode. In order to perform XRD and EXAFS measurements on the same sample, a diffractometer was mounted between the first and the second ionization chamber in the EXAFS spectrometer (*19, 20*). This enabled us to record X-ray diffractograms during an EXAFS measurement simply by interrupting the monochromator scan at a suitable wavelength (1.4 Å in the present work) for the time needed to collect the XRD data and then continuing with the EXAFS scan. The XRD diagrams are obtained using a gas-filled position-sensitive wire detector. In the present setup, the detector covers a region of about $2\Theta = 7°$. In order to achieve an accurate energy calibration of the EXAFS spectra, data of the catalyst and a reference sample (Yb_2O_3), installed between the second and a third ionization chamber, were measured simultaneously.

3. MOLECULAR DYNAMICS SIMULATIONS AND EXAFS ANALYSIS

a. Molecular Dynamics Simulations

The properties of small Cu particles at different temperatures were simulated using a molecular dynamics technique. The interatomic interactions have been described in the effective medium theory, which has been shown to give a good description of the cohesive and surface properties of metals (*21, 22*). Furthermore, the value of the lattice constants is found to agree within a few percent of the crystallographic value. The velocity-Verlet algorithm was used for propagating in time. For details of the molecular-dynamics program, see Ref. (*23*). The particles studied were in the range 256 to 16727 atoms corresponding to diameters of about 17 to 70 Å. The large 16727 atom particle was simulated on a massively parallel Connection-Machine CM-200 computer (*24*). The particles were initially run at high temperature. The temperature was subsequently lowered in steps after the particles had reached their equilibrium crystal shape at each temperature. For all the particles with the sizes studied here, the atoms were found to be arranged in a fcc structure. This compares well with other experimental results for small Cu particles (*25*).

The pair distribution function was calculated as an average over 100 configurations from 14-ps simulations. Only the pair distribution functions for the first shell are considered in the following.

b. EXAFS Analysis Procedures

The generalized EXAFS equation for the case of a continuous radial distribution function, $g(r)$, in the single-scattering, plane-wave approximation is

$$\chi(k) = \frac{F(k)}{k} \int \frac{g(r)}{r^2} \cdot \exp(-2r/\lambda(k)) \cdot \sin(2kr + \phi(k))\, dr, \quad (1)$$

where $F(k)$ is the backscattering amplitude, r is the interatomic distance, k is the wave vector, $\lambda(k)$ is the electron mean free path, and $\phi(k)$ is the total phase shift. The single-scattering approximation is a good approximation when only the first shell is analyzed. Furthermore, errors introduced by using the plane-wave approximation tend to cancel when experimental amplitude and phase functions are transferred from reference compounds also analyzed by the plane-wave approximation.

In the standard EXAFS formalism, originally derived by Sayers *et al.* (*26*), a Gaussian pair distribution function, characterized by the Debye–Waller factor, σ, is assumed and the EXAFS formula for the first shell becomes

$$\chi(k) = A(k) \cdot \sin(\Psi(k)), \qquad (2)$$

where the amplitude and the phase of the EXAFS oscillations are given by

$$A(k) = \frac{N}{kR^2} \cdot F(k) \cdot \exp(-2R/\lambda(k)) \cdot \exp(-2k^2\sigma^2) \qquad (3)$$

$$\Psi(k) = 2kR + \phi(k) \qquad (4)$$

and R is the mean interatomic distance.

For systems with pair distribution functions that deviate from a Gaussian shape, the cumulant expansion approach introduced by Bunker (*27*) is often used and the amplitude and the phase functions in Eq. (2) then become

$$A(k) = \frac{N}{kR^2} \cdot F(k) \cdot \exp(-2R/\lambda(k)) \cdot \exp(-2k^2\sigma^2 + 2/3C_4k^4 - \cdots) \qquad (5)$$

$$\Psi(k) = 2kR + \phi(k) - 4/3C_3k^3 + \cdots, \qquad (6)$$

where C_3, C_4, $\cdots$ are the third-, fourth-, and higher-order cumulants, which are a measure of the deviation of the pair distribution function from a Gaussian shape.

The so-called calculated EXAFS spectra, referred to in the following, are the EXAFS spectra corresponding to the pair distribution functions determined from the molecular dynamics simulations. The $\chi(k) \cdot k$ for the first shell was derived by use of Eq. (1), and the theoretical phase and amplitude functions given by Teo and Lee (*28*) and McKale *et al.* (*29*) were used for $\phi(k)$ and $F(k)$, whereas for the mean free path, $\lambda(k)$, an approximative form given by Teo (*30*) was used. The calculated spectra are then curve fitted using both the standard EXAFS formalism, Eqs. (2) to (4), and the cumulant expansion approach, Eqs. (2), (5), and (6). In the curve fitting, the total phase shift and the normalized amplitude are transferred from the calculated spectrum for bulk Cu metal at the same temperature.

The procedure described in Ref. (*31*) was used to isolate the EXAFS oscillations from the experimentally recorded spectra. In short, this procedure consists of a background removal (cubic spline functions), multiplication by the wave vector k, and normalization. The EXAFS signal is then Fourier transformed, and the contribution from the first coordination shell is complex back Fourier transformed, resulting in a filtered $\chi(k) \cdot k$ spectrum, which was curve fitted analogous to the calculated spectra.

4. RESULTS AND DISCUSSION

a. Molecular Dynamics Simulations

Figure 1 shows typical examples of the atomic arrangement for the 1072- and 16727-atom particles determined by the molecular dynamics simulations. Essentially all low-index planes are observed on the surface of the particles with the (111) plane being the predominant one. Whereas the large particle displays a shape that is close to spherical, the truncation of the facets of the small particles typically gives shapes that deviate significantly from a sphere. Thus, in this case the particle size cannot unambiguously be defined in terms of one dimension only. This aspect will be discussed in a forthcoming publication (*32*). In the present work, we define for simplicity the particle size as the side-length of a cube having its center of mass coinciding with that of the particle and with a size that precisely encloses all the atoms of the particle. Figure 2 shows the relation between the to-

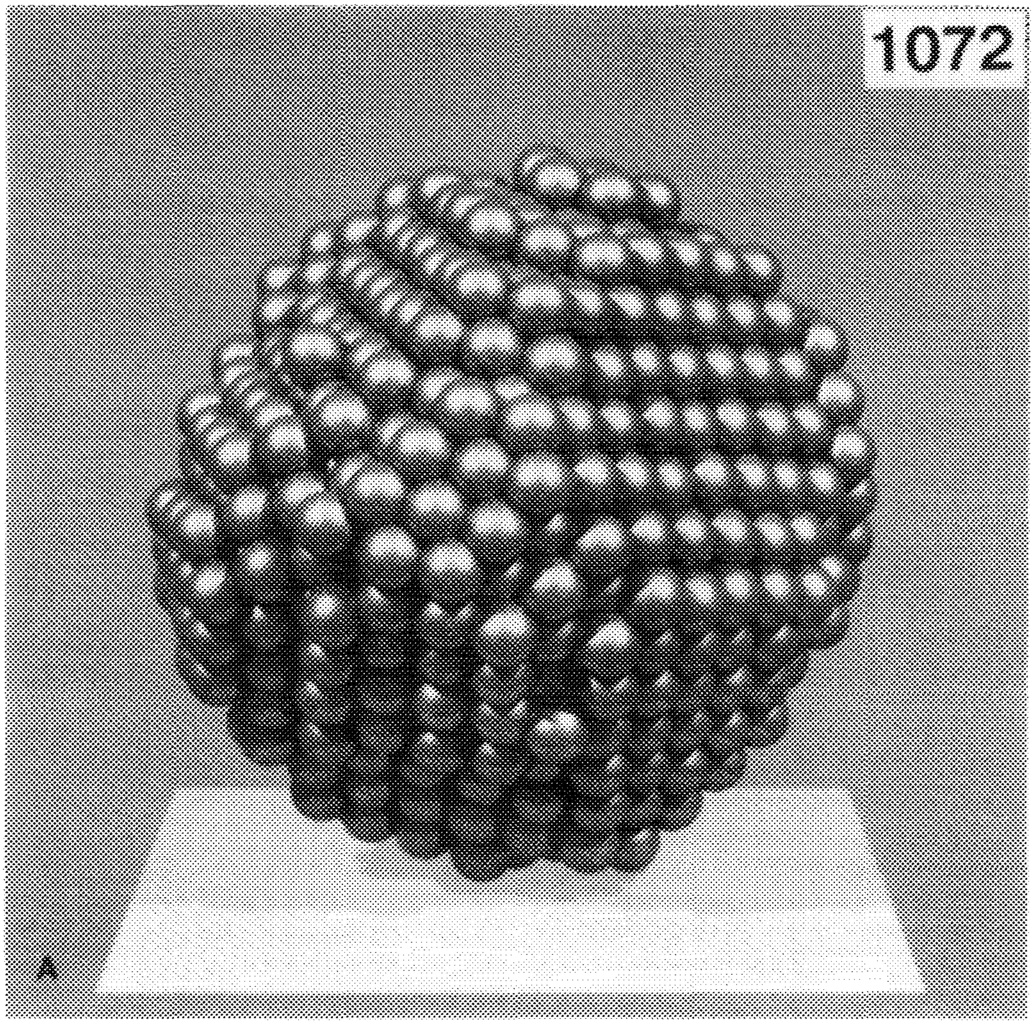

FIG. 1. Graphical representation of the atomic arrangements of the (A) 1072- and (B) 16727-atom Cu particles.

tal number of atoms in the particle and the particle size according to this definition.

In Figure 3 we have plotted the average coordination number from the molecular dynamics simulations as a function of the particle size. Comparing these results with relations obtained from simple geometrical models (*3*, *4*), it is noteworthy that the present model gives values for the coordination numbers that are smaller than those given in Ref. (*3*) but larger than those in Ref. (*4*) for the same particle size.

The advantage of the present approach for relating coordination numbers to particle sizes is that the molecular dynamics simulations directly give both the shape of the particles and the coordination numbers for every atom in the particles. Thus, unlike the previous models [see, e.g. Refs. (*3*, *4*)], various assumptions about shape and distribution of surface planes are not necessary to include.

The normalized Cu–Cu pair distribution functions, $g(r)/r^2$, from the molecular dy-

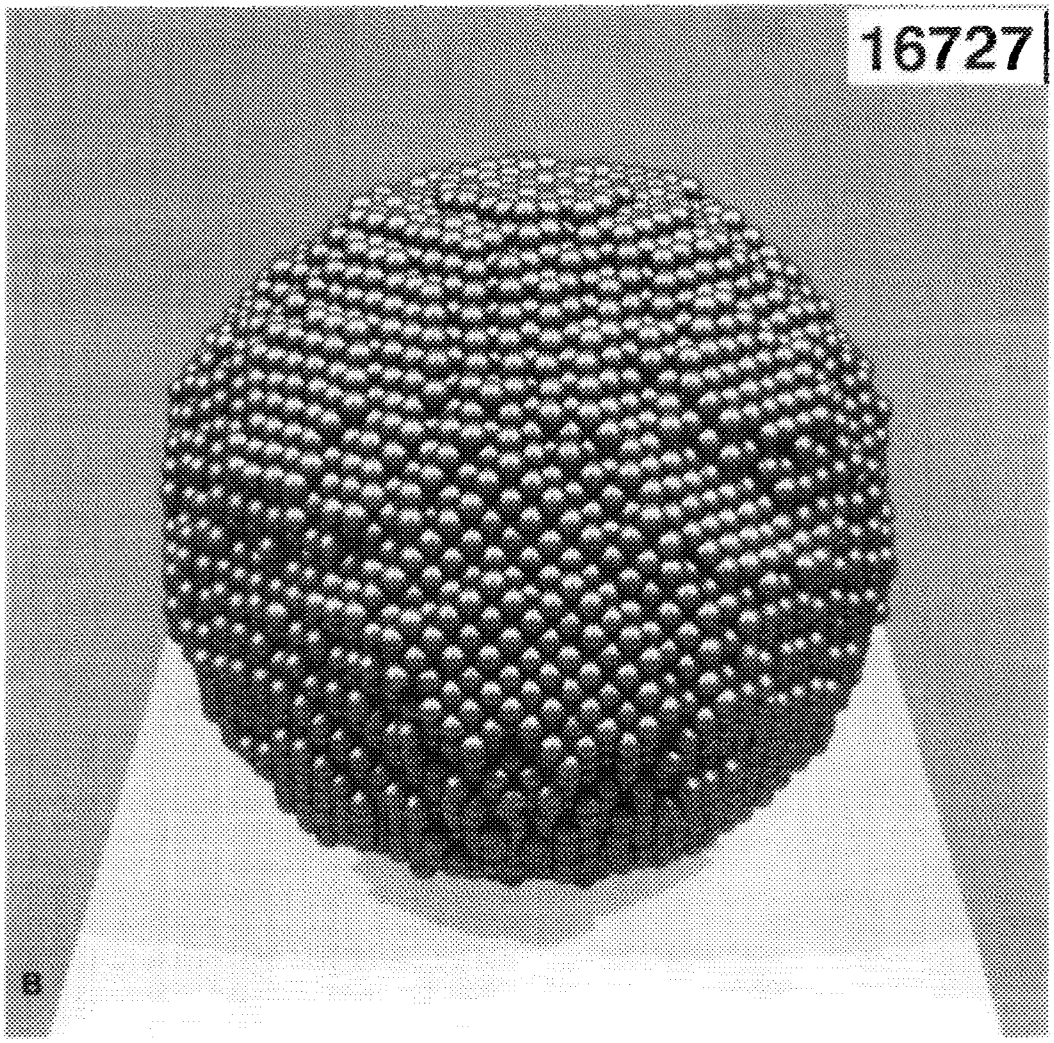

FIG. 1—*Continued*

namics simulations for bulk Cu metal and for particles with 256, 1072, and 16727 Cu atoms (corresponding to particle diameters of about 17, 29, and 70 Å) are shown in Fig. 4. An inspection of the curves reveals that the shape changes from the expected Gaussian-like distribution for bulk Cu to a quite asymmetric distribution with long tails for the small particles. This change is due to an increasing contribution in the small particles of the surface region where the Cu atoms move in a very anharmonic potential (*15*).

b. EXAFS Derived from Molecular Dynamics Simulations

Eisenberger and Brown (*9*) have previously pointed out the serious limitations of the EXAFS technique for studying systems in which the pair distribution function is non-Gaussian. The problems arise from two related sources. The first is the problem of a correct theoretical treatment of EXAFS spectra of systems with complicated pair distribution functions. One attempt to minimize this problem is to use the

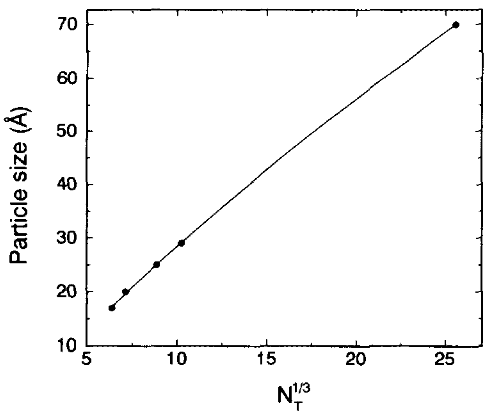

FIG. 2. Relationship between total number of Cu atoms, N_T, and the particle diameter as determined from molecular dynamics simulations.

cumulant expansion approach (*27*) instead of the standard harmonic approach. The second source is due to the loss of information at low *k*-values in experimental EXAFS spectra, a problem that is not easy to solve without relying on model dependent descriptions of the assumed pair distribution function for the actual system. In the following, we address these problems in more detail and show how the molecular dynamics simulations may conveniently overcome the limitations.

In experimentally measured EXAFS spectra, the small *k*-part (up to about 3 $Å^{-1}$) is complicated by multiple scattering, insufficient removal of the atomic absorption, life time broadening of the exited state, etc. Therefore, this part of the experimental spectrum is not included in the normal EXAFS analysis. The magnitude of the errors introduced by omitting this *k*-region can be estimated by comparing the coordination numbers from an analysis of the calculated EXAFS spectra over this *k*-region with the coordination numbers obtained from the molecular dynamics simulations. The average coordination numbers derived from the analysis over the experimentally available *k*-region are termed the "apparent" coordination numbers in contrast to the "true" coordination numbers obtained from the molecular dynamics simulations.

The calculated EXAFS spectra, which are based on the pair distribution functions as derived from the molecular dynamics simulations, can now be used to test the different EXAFS formalisms (see Section 3b). The results of the various fitting procedures are given in Figs. 5 to 7, which show relations between the apparent coordination number determined from the EXAFS analysis and the true coordination number determined from the molecular dynamics simulations. The curve fitting was carried out by use of modified amplitude and total phase functions from the spectrum of bulk

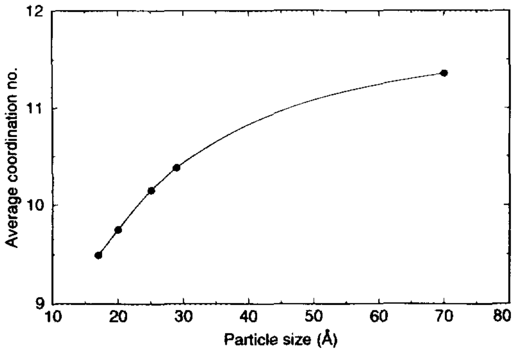

FIG. 3. Average coordination numbers calculated from the molecular dynamics simulations shown as a function of the Cu particle size.

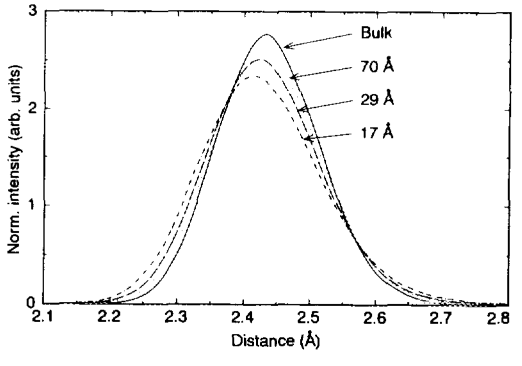

FIG. 4. Normalized pair distribution functions, $g(r)/r^2$, at 280 K for the first shell of bulk Cu and Cu particles with 256 (17 Å), 1072 (29 Å), and 16727 (70 Å) atoms.

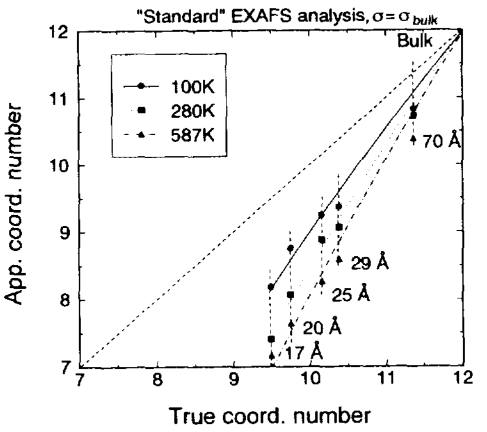

FIG. 5. Relation between the apparent first shell coordination number determined from the standard EXAFS analysis [Eqs. (2) to (4) in the text] and the true coordination number determined from molecular dynamics simulations. The Debye–Waller factor has been kept equal to the bulk value in the curve fitting.

Cu, also derived from the molecular dynamics simulations. The curves in Fig. 5 were obtained using the standard EXAFS formalism, Eqs. (2) to (4), with the Debye–Waller term, $e^{-2k\sigma^2}$, constrained to be identical to that of bulk Cu at the same temperature. A priori one would find this to be a reasonable assumption if the thermal vibrations of the atoms in the small particles were the same as in the bulk. However, the apparent coordination numbers are found to be systematically too small compared to the true values, especially for the smallest particles. The deviation becomes increasingly severe with increasing temperature. Somewhat higher apparent coordinations numbers could be obtained by allowing the Debye–Waller factor to be an adjustable parameter in the fits (Fig. 6), but still the coordination numbers are significantly lower than the true values. The results presented in Figs. 5 and 6 indicate that the Debye–Waller factor (or thermal vibrations) of the atoms is larger in the small particles than in the bulk at the same temperature. The failure to obtain coordination numbers similar to the true values even with the Debye–Waller factor as a fitting parameter also indicates that the pair distribution functions for the small particles deviate from the Gaussian shape found in bulk Cu.

The cumulant formalism, Eqs. (2), (5), and (6), is often used to try to describe EXAFS of systems with pair distribution functions that deviate from a Gaussian shape. By including up to the fifth moment, the results given in Fig. 7 were obtained from the fitting procedure. Attempts to include higher-order cumulants were not found to improve the fits. Compared to the standard EXAFS formalism, the cumulant analysis gives apparent coordination numbers that are closer to the true values. The fact that the cumulant analysis results in a better agreement with the true values for the coordination numbers compared to the standard analysis shows that one cannot assume simple amplitude transferability for systems with differing pair distribution functions (bulk versus small particles).

It should be emphasized that although the cumulant analysis, having more free parameters, gives a better representation of the pair distribution functions for the small particles it will never be able to retrieve the information lost in excluding the low k-part

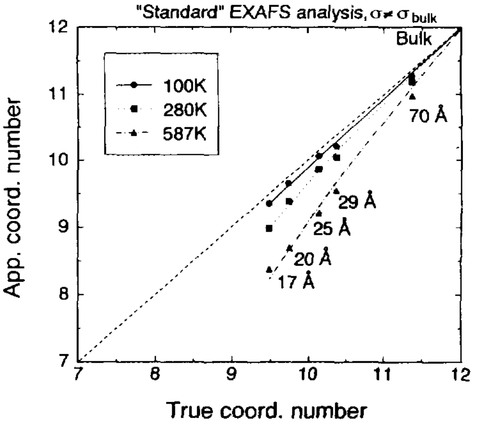

FIG. 6. Relation between apparent first shell coordination number determined from the standard EXAFS analysis and the true coordination number. The results in this figure were obtained with the Debye–Waller factor as an adjustable parameter.

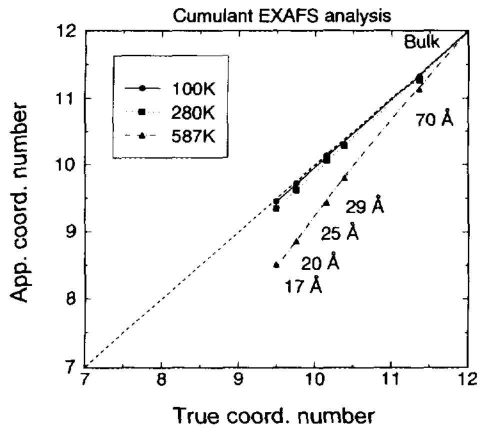

FIG. 7. Relation between the true coordination number and the apparent first shell coordination number determined from an EXAFS analysis using the cumulant formalism [Eqs. (2), (5), and (6) in the text] with up to the fifth moment.

of the experimental spectra. This is the main reason that the EXAFS coordination numbers determined by the cumulant approach are still too low for the highest temperatures. The physical reason for this effect is that the broad tails extending to high and low r-values of the pair distribution function for the small particles will contribute to EXAFS mostly at low k-values, whereas the sharp features of the distribution will be evident at high k-values. Since the anharmonicity of the motion of the Cu atoms becomes increasingly important with increasing temperature, the underestimation of the EXAFS coordination number will accordingly increase with increasing temperature.

The determination of the coordination number can thus be significantly in error because of the combined effect of the loss of the small k-region information and the different shape of the EXAFS amplitude function between the small particles and the bulk Cu reference. The deviation of the apparent coordination numbers from the true values depends on the exact k-region used and on the specific fitting procedure used. Why the error increases significantly when higher cutoff values are used (for example in order to get rid of complicated features near the edge) and when the EXAFS is weighted with high power of k to emphasize the signal at high k-values is discussed in detail elsewhere (*16*).

The fact that the analyses of the particles at 100 K give more reliable coordination numbers originates from the relative small influence of anharmonicity on the atomic motion at low temperatures. Obviously, these results suggest that EXAFS experiments should always be carried out at very low temperatures where the influence of thermal motion is less important.

The need for carrying out the experiments at as low temperature as possible is of course unfortunate since the dynamic nature of the catalyst structure implies a demand for performing *in situ* studies at the reaction temperature. Thus, there is always the possibility that EXAFS studies carried out at low temperatures may not provide a correct structural picture of the working catalyst. Therefore, high-temperature EXAFS spectra are necessary and the present model may provide a mean to give more reliable information from such studies.

The relations between the apparent and true coordination numbers (Figs. 5 to 7) are based on simulations for Cu, but the general principles will also be valid for other metals and work is performed presently to extend the model. Surface anharmonicity is also expected to play a role in nonmetallic systems, like oxides and sulfides, but quantitatively the effect is expected to be different from that found for the metals.

The above simulations are based on the equilibrium shape for free particles, i.e., in the absence of any interaction with gases, supports, or other phases. Such effects, which are currently being investigated, will clearly influence, among others, the equilibrium shape of the crystallites and the distribution of facets on the surface. Thus, although qualitatively the same effects as those described in the present work will be

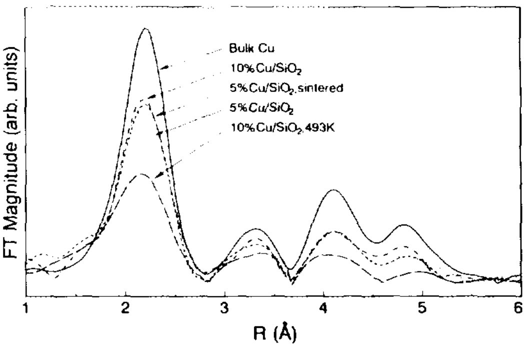

FIG. 8. Fourier transforms of the EXAFS for Cu metal and the Cu/SiO$_2$ catalysts in the reduced state.

present, the quantitative corrections may be different.

c. Comparison with EXAFS and XRD Experiments

In this section we test the quality of the new model for obtaining EXAFS coordination numbers and particle sizes by comparing with the particle sizes obtained from XRD experiments performed by use of the novel, combined XRD/EXAFS setup described in Refs. (*19*, *20*).

Figure 8 shows the Fourier transforms of the EXAFS for bulk copper metal and the silica-supported Cu particles. The data for the silica-supported Cu particles display essentially the same features as metallic copper, but the relative intensity of the peaks is significantly reduced.

The reduced peak amplitudes for the different catalysts show that these contain small copper crystallites. A standard EXAFS analysis in which the Debye–Waller factor was kept equal to that of the bulk gives the apparent coordination numbers listed in Table 1. By use of the geometrical shape model by Greegor and Lytle (*3*) for spherical shaped particles, it is estimated that the Cu particle sizes for the catalysts are in the range from 10 to 12 Å (Table 1). Figure 9 shows the X-ray diffractograms of the same samples as those given in Fig. 8. The presence of a relatively broad Cu(111) line for all the catalysts is observed. From a line profile analysis, the average XRD crystallite sizes listed in Table 1 can be estimated using the Debye–Scherrer formula with the Scherrer constant equal to 0.9. It is clear that these values are significantly larger than those found from the standard EXAFS analysis. Since the XRD and the EXAFS data have been collected on the *same* sample under *identical* conditions, it can be ruled out that this discrepancy is due to different treatments of the catalysts. Quantitative XRD

TABLE 1

Apparent Coordination Numbers and Estimated Particle Diameters for Silica-Supported Cu Catalysts

Catalyst	Apparent coordination number ($\sigma = \sigma_{\text{bulk}}$)	*D* (Å)		
		Geometrical model [Ref. (*3*)]	XRD[a]	New method (Fig. 5)
5% Cu/SiO$_2$, 300 K	8.7	11.0	27	24
5% Cu/SiO$_2$[b], 300 K	9.3	12.0	39	34
10% Cu/SiO$_2$, 300 K	9.0	11.5	35	28
10% Cu/SiO$_2$, 493 K	8.5[c]	10.5	30	26

[a] Uncertainties of the XRD results, about ±5 Å.

[b] Sintered catalyst.

[c] Bulk Cu metal reference also measured at 493 K.

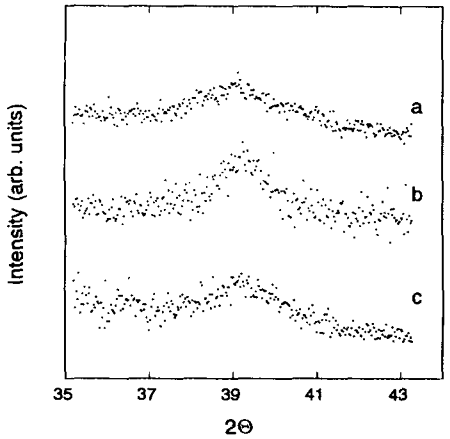

FIG. 9. X-ray diffractograms showing the Cu(111) line in (a) 5% Cu/SiO$_2$, (b) sintered 5% Cu/SiO$_2$, and (c) 10% Cu/SiO$_2$ catalysts recorded using the combined XRD/EXAFS setup; i.e., the data in Figs. 8 and 9 were recorded on the *same* sample in the *same* cell.

studies of selected samples also rule out that the difference can be explained by the presence of a large amount of particles being too small to be observed by XRD. Also, independent studies by use of the newly developed H$_2$-TPD technique (*33*) confirm that the standard EXAFS analysis severely underestimates the particle sizes.

A much better agreement is obtained, however, if we use the new procedure for correcting the apparent coordination numbers (Fig. 5) and the coordination number–particle size relationship given in Fig. 3. The particle sizes obtained by this method (Table 1) show much better agreement with the XRD results.

5. CONCLUSION

The present results show that the determination of particle sizes in highly dispersed systems by EXAFS is not a straightforward procedure. The fact that the motion of the atoms in the surface regions of the small particles is very anharmonic, especially at high temperatures, gives rise to asymmetric pair distribution functions with broad tails that contribute at the low k-region of the EXAFS spectrum. The contribution from such effects thus increases with decreasing particle size. Due to the loss of the low k-part of the experimentally measured EXAFS spectrum and the nontransferability of amplitude functions between the reference bulk material and the small particles, the obtained coordination numbers will systematically be too small. However, the present molecular dynamics simulations allow one to directly calculate the errors introduced by not having access to the low k-part of the EXAFS spectrum. Thus, one of the results of the present work is a model and a procedure whereby more reliable coordination numbers can be estimated from EXAFS experiments. Moreover, since the molecular dynamics simulations provide direct relationships between coordination numbers and particle sizes, more reliable sizes will also result as indeed confirmed by XRD and other experiments.

The errors in the coordination numbers are less important when EXAFS experiments are carried out at low temperature. However, at such temperatures the state of the catalysts may not be the same as at reaction conditions. Furthermore, by restricting ourselves to low-temperature experiments, we also prevent dynamic studies of, for example, activation and sintering phenomena to be carried out. Thus, there is a great desire to record EXAFS spectra at high temperature at which the catalysis takes place. At these temperatures, the errors from the EXAFS analysis of small particles are quite significant and the present model therefore especially important to apply. Although the present results were obtained for Cu, it is expected that the conclusions also hold for small particles of other metals.

The influence of anharmonicity is expected to be especially important in SEXAFS experiments where one exclusively probes the surface. Thus, surface structural models based on SEXAFS bond lengths and coordination numbers without correcting for the influence of anharmonicity may need some reconsideration in light of the present results.

ACKNOWLEDGMENTS

Financial support from the Danish Research Councils through the Center for Surface Reactivity is gratefully acknowledged. The Connection Machine resources at UNI-C were provided through the Center for Parallel Computer Research (CAP) funded by the Danish Natural Science Research Council. The authors are grateful to HASYLAB for offering beam time at the RÖMO II experimental station. We also thank G. Steffensen and P. L. Hansen for experimental assistance and B. S. Hammershøi for preparing the samples.

REFERENCES

1. Delgass, W. N., Haller, G. L., Kellerman, R., and Lunsford, J. H., Eds., "Spectroscopy in Heterogeneous Catalysis." Academic Press, New York, 1979.

2. Thomas, J. M., and Lambert, R. M., Eds., "Characterization of Catalysts." Wiley, New York, 1980.

3. Greegor, R. B., and Lytle, F. W., *J. Catal.* **63,** 476 (1980).

4. Kip, B. J., Duivenvoorden, F. B. M., Koningsberger, D. C., and Prins, R., *J. Catal.* **105,** 26 (1987).

5. Boudart, M., and Meitzner, G., *in* "EXAFS and Near Edge Structure III" (K. O. Hodgson, B. Hedman, and J. E. Penner-Hahn, Eds.), p. 217. Springer-Verlag, Berlin, 1984.

6. Davis, R. J., Landry, S. M., Horsley, J. A., and Boudart, M., *Phys. Rev. B* **39,** 10580 (1989).

7. Shaw, E. A., Rayment, T., Walker, A. P., Lambert, R. M., Gauntlett, T., Oldman, R. J., and Dent, A., *Catal. Today* **9,** 197 (1991).

8. Couves, J. W., Thomas, J. M., Waller, D., Jones, R. H., Dent, A. J., Derbyshire, G. E., and Greaves, G. N., *Nature* **354,** 465 (1991).

9. Eisenberger, P., and Brown, G. S., *Solid State Commun.* **29,** 481 (1979).

10. Eisenberger, P., and Lengeler, B., *Phys. Rev. B* **22,** 3551 (1980).

11. Marques, E. C., Sandstrom, D. R., Lytle, F. W., and Greegor, R. B., *J. Chem. Phys.* **77,** 1027 (1982).

12. Lamble, G., and King, D. A., *Philos. Trans. R. Soc. London, Ser. A* **318,** 203 (1986).

13. Freund, J., Ingalls, R., and Crozier, E. D., *Phys. Rev. B* **39,** 12537 (1989).

14. Magnan, H., Chandesris, D., Rossi, G., Jezequel, G., Hricovini, K., and Lecante, J., *Phys. Rev. B* **40,** 9989 (1989).

15. Hansen, L. B., Stoltze, P., Nørskov, J. K., Clausen, B. S., and Niemann, W., *Phys. Rev. Lett.* **64,** 3155 (1990).

16. Clausen, B. S., Topsøe, H., Hansen, L. B., Stoltze, P., and Nørskov, J. K., *Jpn. J. Appl. Phys.*, in press.

17. van Dillen, J. A., Geus, J. W., Hermans, L. A. M., and van der Meijden, J., *in* "Proceedings, 6th International Congress on Catalysis, London, 1976" (G. C. Bond, P. E. Wells, and F. C. Tompkins, Eds.), p. 677. The Chemical Society, London, 1976.

18. Clausen, B. S., Steffensen, G., Fabius, B., Villadsen, J., Feidenhans'l, R., and Topsøe, H., *J. Catal.* **132,** 524 (1991).

19. Clausen, B. S., Gråbæk, L., Steffensen, G., and Topsøe, H., "HASYLAB Annual Report," p. 495. 1991.

20. Clausen, B. S., Gråbæk, L., Steffensen, G., Hansen, P. L., and Topsøe, H., *Catal. Lett.*, submitted.

21. Jacobsen, K. W., Nørskov, J. K., and Puska, M. J., *Phys. Rev. B* **35,** 7423 (1987).

22. Jacobsen, K. W., *Comments Cond. Mat. Phys.* **14,** 129 (1988).

23. Stoltz, P., *J. Chem. Phys.* **92,** 6309 (1990).

24. Nielsen, O. H., Sethna, J. P., Stoltze, P., Jacobsen, K. W., and Nørskov, J. K., to be published.

25. Montano, P. A., Shenoy, G. K., Alp, E. E., Schulze, W., and Urban, J., *Phys. Rev. Lett.* **56,** 2076 (1986).

26. Sayers, D. E., Stern, E. A., and Lytle, F. W., *Phys. Rev. Lett.* **27,** 1204 (1971).

27. Bunker, G., *Nucl. Instrum. Methods* **207,** 437 (1983).

28. Teo, B.-K., and Lee, P. A., *J. Am. Chem. Soc.* **101,** 2815 (1979).

29. McKale, A. G., Veal, B. W., Paulikas, A. P., Chan, S.-K., and Knapp, G. S., *J. Am. Chem. Soc.* **110,** 3763 (1988).

30. Teo, B.-K., *J. Am. Chem. Soc.* **103,** 3990 (1981).

31. Niemann, W., Malzfeldt, W., Rabe, P., Haensel, R., and Lübcke, M., *Phys. Rev. B* **35,** 1099 (1987).

32. Hansen, L. B., Stoltze, P., Nørskov, J. K., Clausen, B. S., and Topsøe, H., to be published.

33. Muhler, M., Nielsen, L. P., Törnqvist, E., Clausen, B. S., and Topsøe, H., *Catal. Lett.* **14,** 241 (1992).